Bat Algorithm for Automatic Chaos Control Method Driven by Multiplicative Pulses to the System Variables on the Logistic Map

Akemi Gálvez[1,2][0000-0002-2100-2289], Andrés Iglesias[1,2,†][0000-0002-5672-8274]

[1] Department of Applied Mathematics and Computational Sciences
University of Cantabria, Avenida de los Castros s/n, 39005, Santander, Spain
[2] Faculty of Pharmaceutical Sciences, Narashino Campus
Toho University, 2-2-1 Miyama, 274-8510, Funabashi, Japan
[†]Corresponding author: iglesias@unican.es

Abstract. Chaotic systems are characterized by extreme sensitivity to initial conditions, where two arbitrarily close starting points lead to exponentially divergent trajectories over time. Since the 1990s, research has demonstrated that chaotic behavior can be controlled, a phenomenon known as chaos control. In this paper, we address the problem of chaos control in unidimensional maps, specifically focusing on stabilizing chaotic dynamics to a periodic orbit of a given period. Our approach builds on a previously proposed method that applies control pulses of intensity λ to the system variables every Δn iterations, where λ and Δn are adjustable parameters. We formulate this problem as a challenging multimodal, multivariate, continuous, nonlinear optimization task and tackle it using the bat algorithm, a popular swarm intelligence method. To evaluate the effectiveness of our approach, we conduct computational experiments on the logistic map under various parameter settings. The results indicate that our method performs effectively for all tested chaotic behaviors. We conclude that the proposed approach is a promising step toward an automated procedure for chaos control in chaotic maps.

Keywords: Dynamical systems · chaotic maps · chaos control · continuous optimization · swarm intelligence · bat algorithm

1 Introduction

Dynamical systems are a widely studied research topic due to their ability to describe complex real-world phenomena across various fields, including mathematics, physics, chemistry, engineering, biology, medicine, and economics. Broadly, a dynamical system is defined as a system governed by a mathematical function that describes the temporal evolution of a point in a n-dimensional space, known as the *phase space*. Dynamical systems are classified as either discrete (typically described by difference equations) or continuous (described by differential equations) [2, 40]. Given an initial condition for the system variables,

ICCS Camera Ready Version 2025
To cite this paper please use the final published version:
DOI: 10.1007/978-3-031-97564-6_17

integrating these equations produces a *trajectory* or *orbit* that traces the system evolution [1, 7, 18]. These trajectories serve as a powerful analytical tool for understanding the temporal evolution of the system behavior.

A particularly intriguing class of dynamical systems is *chaotic system*s, which are distinguished by their extreme sensitivity to initial conditions. This sensitivity means that even the smallest perturbations in the starting conditions (e.g., due to measurement noise or numerical rounding errors) can grow exponentially over time, leading to significantly divergent outcomes. Remarkably, this unpredictable behavior arises even in systems governed by purely deterministic equations, a phenomenon known as *deterministic chaos* [20, 34].

Despite their apparent randomness, chaotic systems exhibit underlying structures. For instance, many chaotic systems possess *attractors* – bounded regions in the phase space toward which trajectories tend to evolve. These attractors can take various forms, including fixed points, finite point sets, curves, or more complex fractal structures known as *strange attractors*. Chaotic attractors contain an infinite number of unstable periodic orbits. The chaotic behavior emerges as the system's trajectory moves near one unstable periodic orbit, follows it briefly, and then transitions to another, resulting in an intricate and seemingly unpredictable pattern over time.

For many years, the unpredictable nature of chaotic systems was viewed as problematic and undesirable. However, in 1990, it was demonstrated that chaotic dynamics could be stabilized through small perturbations to system parameters. The first method of this kind, known as the OGY method [28], uses a Poincaré section to identify an unstable periodic orbit. By applying carefully calculated perturbations when the system approaches this orbit, the trajectory can be redirected from the unstable manifold to the stable manifold, thereby stabilizing the chaotic system [35]. Since the introduction of the OGY method, numerous other chaos control techniques have been developed, including the time-delayed feedback method proposed by Pyragas [31]. Other examples of chaos control techniques can be found in [3, 5, 26, 30, 32, 33, 36]. Comprehensive surveys on chaos control methods can be found in [4, 6, 8], while experimental validations are reported in [21, 27].

An alternative approach to chaos control involves applying small perturbations directly to the system variables [15, 16]. This includes methods utilizing pulses applied on Poincaré and Lorenz sections [19, 22]. The general framework involves applying additive or multiplicative discrete pulses of intensity λ at fixed intervals of Δn iterations. Historically, this method has been implemented manually, with parameter selection based on trial and error. Automating this process requires optimizing key parameters, including the pulse intensity λ and frequency Δn, to achieve effective control.

In this paper, we address the automation of chaos control using multiplicative pulses by formulating it as a minimization problem. This formulation presents a significant challenge due to its continuous, multivariate, multimodal, and nonlinear nature, which is not usually handled by conventional optimization techniques. To overcome these difficulties, we employ the bat algorithm, a popular

ICCS Camera Ready Version 2025
To cite this paper please use the final published version:
DOI: 10.1007/978-3-031-97564-6_17

bio-inspired swarm intelligence method. Additionally, to reduce computational complexity, our study focuses on one-dimensional maps.

The paper is organized as follows: Section 2 discusses briefly the chaos control method and the optimization problem. Section 3 introduces the bat algorithm as the selected optimization technique. Section 4 describes the experimental setup and the example used in this study. Section 5 presents and analyzes the computational results. Finally, Section 6 concludes the paper with a summary of findings and potential directions for future research.

2 The Chaos Control Optimization Problem

In [15, 16], it was demonstrated that chaotic behavior can be stabilized by introducing pulses into the system variables. Building on this idea, we consider multiplicative pulses of the form $x_i \rightarrow (1+\lambda)x_i$, where x_i denotes the system variable at iteration i and λ represents the pulse intensity. These pulses are applied every Δn iterations, i.e., when $mod(i, \Delta n) = 0$. The perturbation is maintained for a duration of q iterations, following an initial transient phase of p iterations during which no perturbation is applied. Note that the parameters λ, Δn, p and q are to be determined to achieve the desired system behavior.

Given a chaotic dynamical system and a predefined target periodic orbit, our approach involves optimizing these parameters to drive the system toward the desired periodic state. As mentioned earlier, this formulation results in a highly complex continuous multivariate multimodal nonlinear optimization problem. Even for low-dimensional dynamical systems, solving this problem presents significant challenges that traditional mathematical optimization techniques struggle to address. To overcome this, we employ a bio-inspired swarm intelligence method well-suited for continuous optimization: the bat algorithm. The following section provides a detailed description of this approach.

3 The Bat Algorithm

The *bat algorithm* is a widely used swarm intelligence technique for solving continuous optimization problems, inspired by the echolocation behavior of microbats [41, 43]. Microbats employ echolocation for navigation, prey detection, and obstacle avoidance. The algorithm models these behaviors through a population of agents (referred to as "bats") that explore the search space to locate optimal solutions based on a defined fitness function.

The algorithm begins by randomly initializing a population of bats across the search space. Each bat i at iteration g is characterized by three key parameters: its frequency f_i^g, position $\mathbf{x}_i^g$, and velocity $\mathbf{v}_i^g$, determined by the following equations:

$$f_i^g = f_{min}^g + \beta(f_{max}^g - f_{min}^g) \tag{1}$$

$$\mathbf{v}_i^g = \mathbf{v}_i^{g-1} + \left[\mathbf{x}_i^{g-1} - \mathbf{x}^*\right] f_i^g \tag{2}$$

$$\mathbf{x}_i^g = \mathbf{x}_i^{g-1} + \mathbf{v}_i^g \tag{3}$$

ICCS Camera Ready Version 2025
To cite this paper please use the final published version:
DOI: 10.1007/978-3-031-97564-6_17

Here, β is a uniformly distributed random variable in the range $[0, 1]$, and $\mathbf{x}^*$ represents the current global best solution found by evaluating the fitness of all bats. In addition to global exploration, the algorithm performs a local search around the best solution using a random walk: $\mathbf{x}_{new} = \mathbf{x}_{old} + \epsilon\mathcal{A}^g$, where ϵ is a uniformly distributed random number in $[-1, 1]$, and $\mathcal{A}^g =< \mathcal{A}_i^g >$ denotes the average loudness of all bats at iteration g. New candidate solutions are accepted if they improve the current best solution, with an acceptance probability influenced by the bat's loudness. Upon acceptance, the pulse emission rate r_i and loudness $\mathcal{A}_i$ are dynamically updated according to the following rules: $r_i^{g+1} = r_i^0[1 - \exp(-\gamma g)]$ and $\mathcal{A}_i^{g+1} = \alpha\mathcal{A}_i^g$, where γ and α are user-defined parameters controlling the rate of change. This adaptive mechanism allows the algorithm to balance exploration and exploitation: as the search progresses, bats emit pulses more frequently while their loudness decreases, focusing the search around promising regions. The algorithm iterates until a maximum number of generations, $\mathcal{G}_{max}$, is reached.

Each bat is initialized with random values for loudness $\mathcal{A}_i^0 \in (0, 2)$ and pulse emission rate $r_i^0 \in [0, 1]$, which are updated only when better solutions are found. The bat algorithm is chosen in this work due to its demonstrated effectiveness in handling complex, multimodal optimization problems, as supported by previous research by the authors (e.g., [10, 12–14, 23–25, 37–39]). For a comprehensive overview of the bat algorithm and its applications, readers are referred to [42].

4 Example and Experimental Settings

The proposed method has been applied to various instances of chaotic maps. However, due to space limitations, this paper focuses on a representative example: the logistic map.

4.1 Illustrative example: the logistic map

The logistic map is a well-known one-dimensional chaotic map frequently used in the study of dynamical systems. It is defined by the quadratic difference equation:

$$x_{n+1} = rx_n(1 - x_n) \tag{4}$$

where r is the system parameter. By varying r, the logistic map exhibits a range of dynamic behaviors, which can be effectively visualized through a *bifurcation diagram*. In this diagram, the vertical axis represents the system's attractors, while the horizontal axis corresponds to the parameter r. Figure 1(top) displays the bifurcation diagram of the logistic map for $r \in [0, 4]$. As shown in the graph, the logistic map exhibits a fixed-point orbit for $0 \leqslant r < 3$. Specifically, the value of the fixed point is zero for $0 \leqslant r < 1$ and $(r - 1)/r$ for $1 \leqslant r < 3$. For $r = 3$ the system exhibits a period-doubling bifurcation where the fixed-point orbit is replaced by a periodic orbit of period-2. This period-doubling bifurcation process continues for larger values of r, and periodic orbits of periods 2, 4, 8, 16, and so on are obtained. This process is a typical route to chaos

ICCS Camera Ready Version 2025
To cite this paper please use the final published version:
DOI: 10.1007/978-3-031-97564-6_17

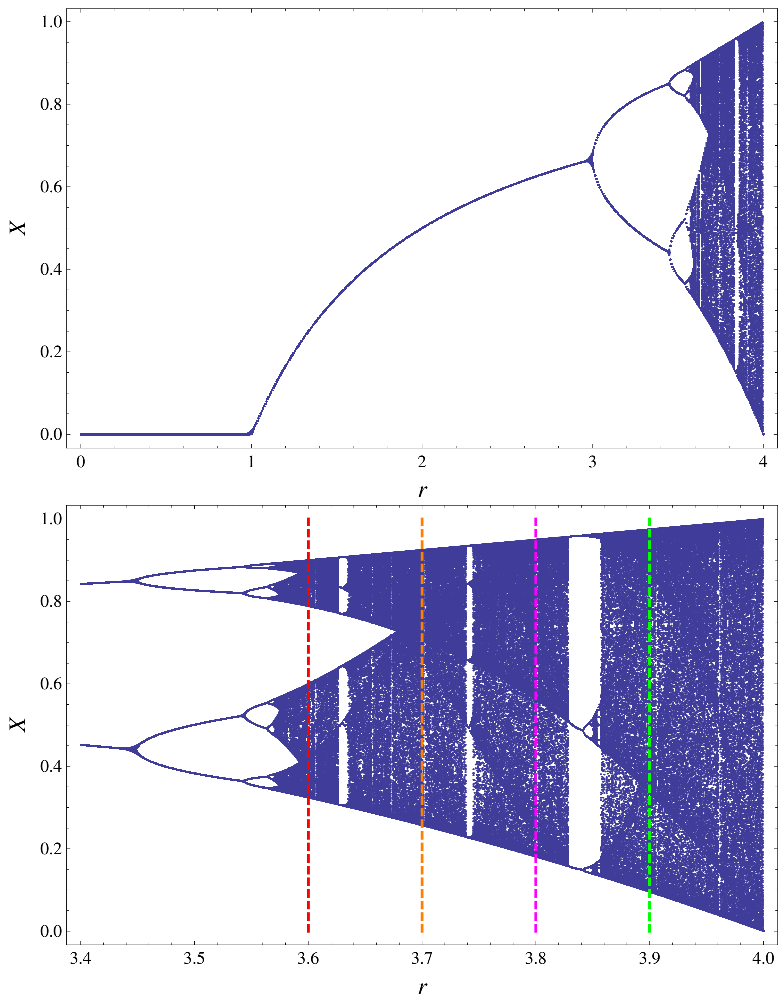

Fig. 1. Bifurcation diagram of the logistic map for the interval $r \in [0, 4]$ (top), and magnification of the diagram on the interval $r \in [3.4, 4]$ (bottom).

known as the period doubling cascade. This chaotic behavior emerges for the parameter value $r_\infty = 3.46994...$. Increasing the value of r even further, the system exhibits chaotic behavior until the value $r = 4$, with some windows of periodicity arisen for certain interval values of r. This behavior can be better seen in Fig. 1(bottom) which shows a magnification of the bifurcation diagram on the interval $r \in [3.4, 4]$. In this paper we focus on four parameter values within the chaotic regime: $r_1 = 3.6$, $r_2 = 3.7$, $r_3 = 3.8$ and $r_4 = 3.9$. These values are highlighted in Figure 1(bottom) by the four vertical dashed lines in red, orange, magenta, and green, respectively.

ICCS Camera Ready Version 2025
To cite this paper please use the final published version:
DOI: 10.1007/978-3-031-97564-6_17

Table 1. Best values of the pulse intensity λ and pulse frequency Δn for the parameter r and the target periods *per* in all the examples presented in the figures of this paper.

r	*per*	λ	Δn	r	*per*	λ	Δn	r	*per*	λ	Δn	r	*per*	λ	Δn
3.6	1	-0.31	1	3.7	1	-0.2	1	3.8	1	-0.45	1	3.9	1	-0.43	1
	3	-0.31	3		2	-0.1	1		2	-0.9	2		2	-0.87	2
	4	0.25	2		3	-0.3	3		4	-0.45	2		4	-0.55	4
	5	0.039	1		4	-0.05	1		4	-0.41	4		6	-0.79	3
	8	-0.31	2		6	-0.22	2		6	-0.45	3		7	-0.52	4
	12	0.019	1		12	-0.3	2		6	-0.9	3		8	-0.49	4

4.2 Experimental Settings

To apply the bat algorithm to our optimization problem, it is essential to define an appropriate representation of individuals and to fine-tune the algorithm parameters. In our approach, each individual $\mathcal{B}_i^k$ of index i at iteration k, representing potential solutions of the problem, is given by a vector: $\mathcal{B}_k = (\lambda_i^k, \Delta_i^k, p_i^k, q_i^k)$, where λ_i^k takes real values on the interval $(-1, 1)$, Δ_i^k is a positive integer ranging from 1 to 5, and p_i^k, q_i^k can take integer values from 500 to 5,000. However, our experiments indicate that p_i^k and q_i^k have minimal influence on the performance of the method. Thus, to reduce the search space and focus on optimizing λ_i^k and Δ_i^k, we fix their values as $p_i^k = q_i^k = 3,000$ in all simulations. A population size of 50 individuals was used in this work.

About the parameter tuning, the bat algorithm is run for a fixed number of iterations, denoted by $\mathcal{G}_{max}$. Based on extensive simulations, we found that $\mathcal{G}_{max} = 100$ iterations provides sufficient convergence across all tested cases. The remaining parameters of the bat algorithm are set empirically as follows: $\mathcal{A}^0 = 0.5$, $r^0 = 0.3$, $\alpha = 0.5$, and $\gamma = 0.25$. Subsequently, the bat algorithm is executed. At the end of the process, the best-performing individual from the final iteration is selected as the solution to the optimization problem.

The computations in this paper have been carried out on a PC desktop with a processor Intel Core i9 running at 3.7 GHz and with 64 GB of RAM. The source code has been developed by the authors in the programming language of the scientific program *Mathematica* version 12.

5 Computational Results

The bat algorithm described in Sect. 3 has been applied to the logistic map presented in Sect. 4.1, using the settings indicated in Sect. 4.2. This section details the computational results obtained for four cases, each corresponding to a different value of the system parameter r. Table 1 summarizes the optimal values of the pulse intensity λ and pulse frequency Δn obtained using our method for all the examples shown in the figures of this paper. It is worth noting that the proposed approach can stabilize a wide range of chaotic behaviors into periodic

ICCS Camera Ready Version 2025
To cite this paper please use the final published version:
DOI: 10.1007/978-3-031-97564-6_17

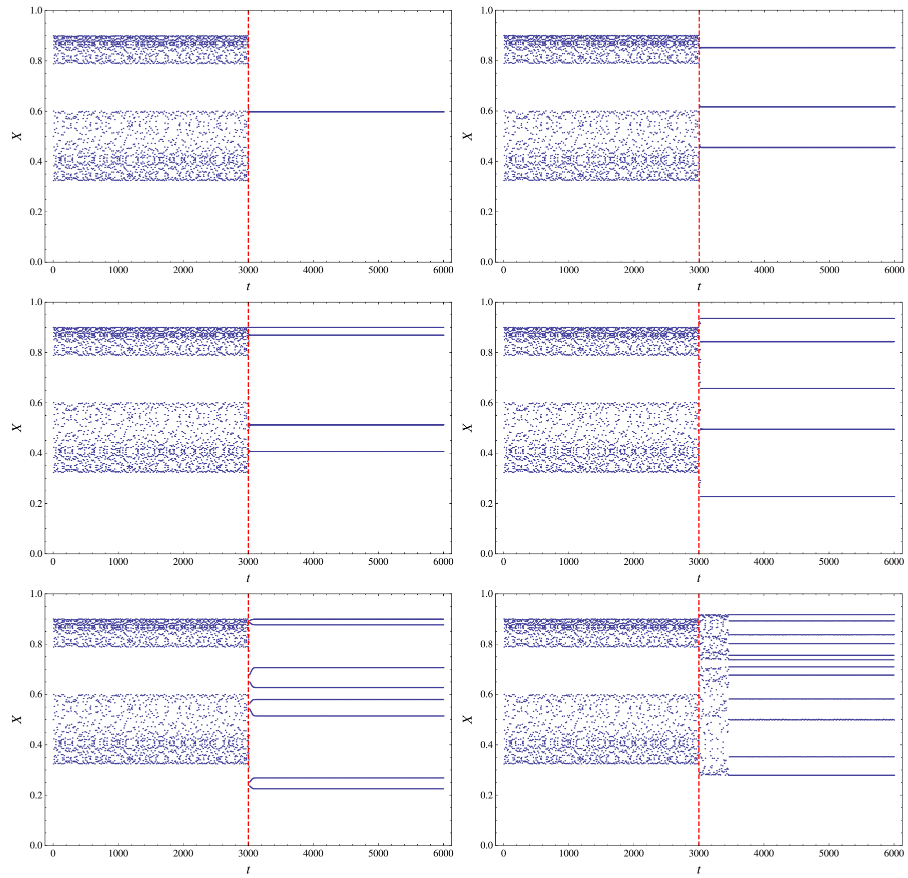

Fig. 2. (top-bottom, left-right) Six examples of application of our method for the logistic map and the parameter value $a = 3.6$: (t-l) period-1 orbit; (t-r) period-3 orbit; (m-l) period-4 orbit; (m-r) period-5 orbit; (b-l) period-8 orbit; (b-r) period-12 orbit.

orbits of a desired period. However, due to space limitations, we focus on a selected set of 24 examples, each representing a different periodic orbit arising from chaotic behavior for various values of r. In our opinion, these examples provide strong evidence of the method's effectiveness and its ability to handle diverse scenarios with consistently satisfactory results.

5.1 Case 1: parameter value $r = 3.6$

Figure 2 presents six examples demonstrating the application of our method to stabilize chaotic orbits of the logistic map for the parameter value $r = 3.6$, for which the logistic map exhibits a two-piece chaotic attractor. In all figures, a vertical red dashed line indicates the time at which the control strategy is applied. As shown in the figures, the method exhibits a very good performance,

ICCS Camera Ready Version 2025
To cite this paper please use the final published version:
DOI: 10.1007/978-3-031-97564-6_17

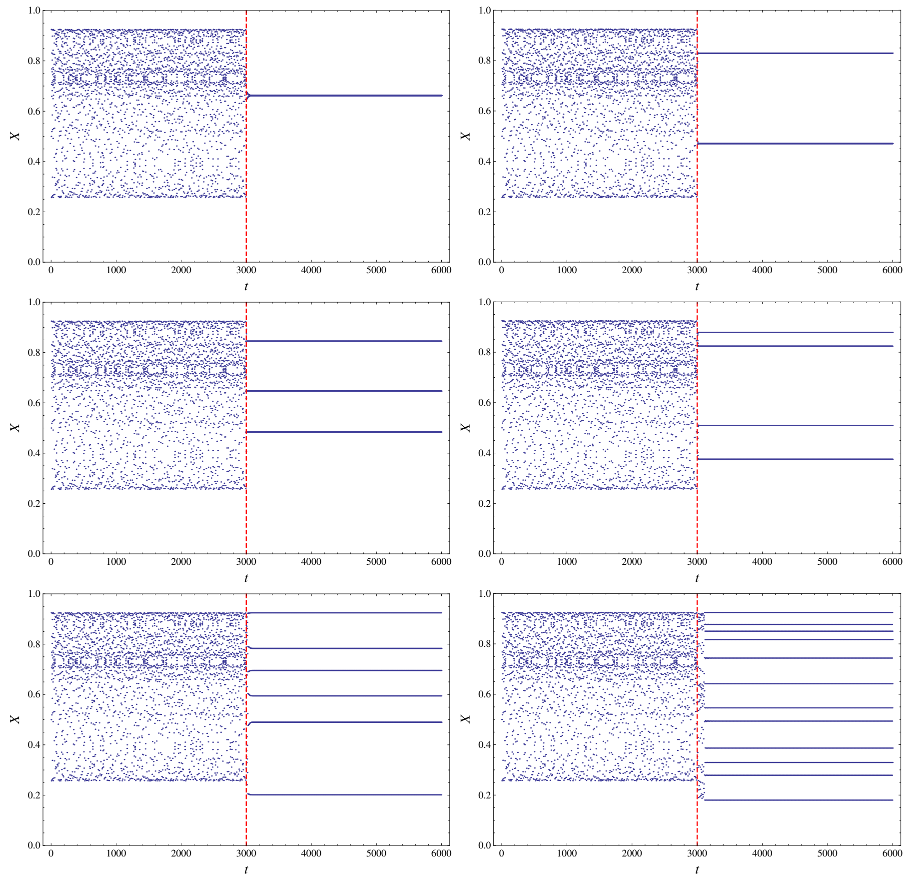

Fig. 3. (top-bottom, left-right) Six examples of application of our method for the logistic map and the parameter value $a = 3.7$: (t-l) period-1 orbit; (t-r) period-2 orbit; (m-l) period-3 orbit; (m-r) period-4 orbit; (b-l) period-6 orbit; (b-r) period-12 orbit.

as we have been able to stabilize the chaotic behavior of the system to periodic orbits of different periods. Notably, periodic orbits of periods 1, 3, 4, 5, 8 and 12 have been obtained automatically using our method, a clear indication of the high flexibility of our approach. Note also that the transient between the chaotic and the periodic behavior is generally very short, with just a few iterations typically needed for convergence to a periodic behavior. The exception is the period-12 orbit in Fig. 2(bottom-right), where a longer transient was required. Nevertheless, even in this challenging case, the system stabilized within 500 iterations. It is also worthwhile to notice that these periodic orbits have been obtained for both positive (periods 4, 5, and 12) and negative (periods 1, 3, and 8) pulse values. Also, we remark that different periodic behaviors (periods 1, 3, and 8) have been obtained for the same pulse intensity, $\lambda = -0.31$, but

ICCS Camera Ready Version 2025
To cite this paper please use the final published version:
DOI: 10.1007/978-3-031-97564-6_17

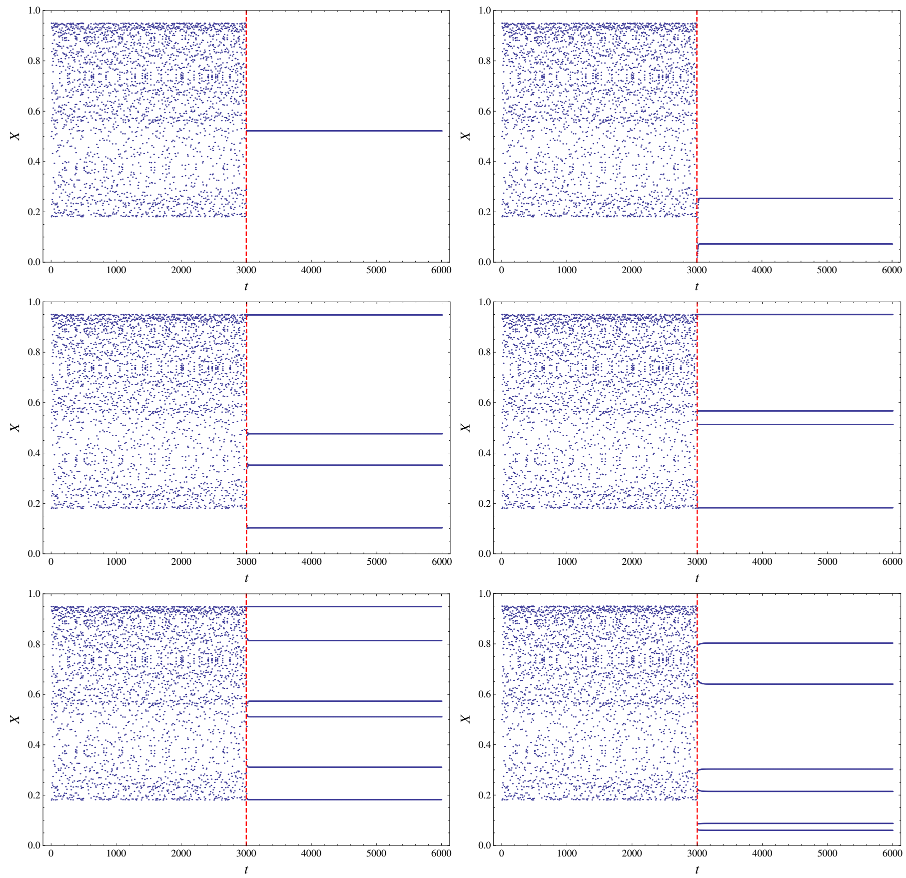

Fig. 4. (top-bottom, left-right) Six examples of application of our method for the logistic map and the parameter value $a = 3.8$: (t-l) period-1 orbit; (t-r) period-2 orbit; (m-l) period-4 orbit; (m-r) period-4 orbit; (b-l) period-6 orbit; (b-r) period-6 orbit.

different pulse frequency ($\Delta n = 1$, $\Delta n = 3$, and $\Delta n = 2$, respectively). This show the great ability of the method to find orbits of different periods through the interplay between these parameters.

5.2 Case 2: parameter value $r = 3.7$

Figure 3 shows six additional examples for the parameter value $r = 3.7$, corresponding to period 1, 2, 3, 4, 6 and 12 orbits selected as targets, respectively. Similar to the previous examples, convergence to the periodic behavior is achieved very quickly once the chaos control method is applied. Note also that the size of the attractor can be enlarged with the chaos control method, even for relatively small values of the pulse intensity, as seen for the period-6 and period-12 or-

ICCS Camera Ready Version 2025
To cite this paper please use the final published version:
DOI: 10.1007/978-3-031-97564-6_17

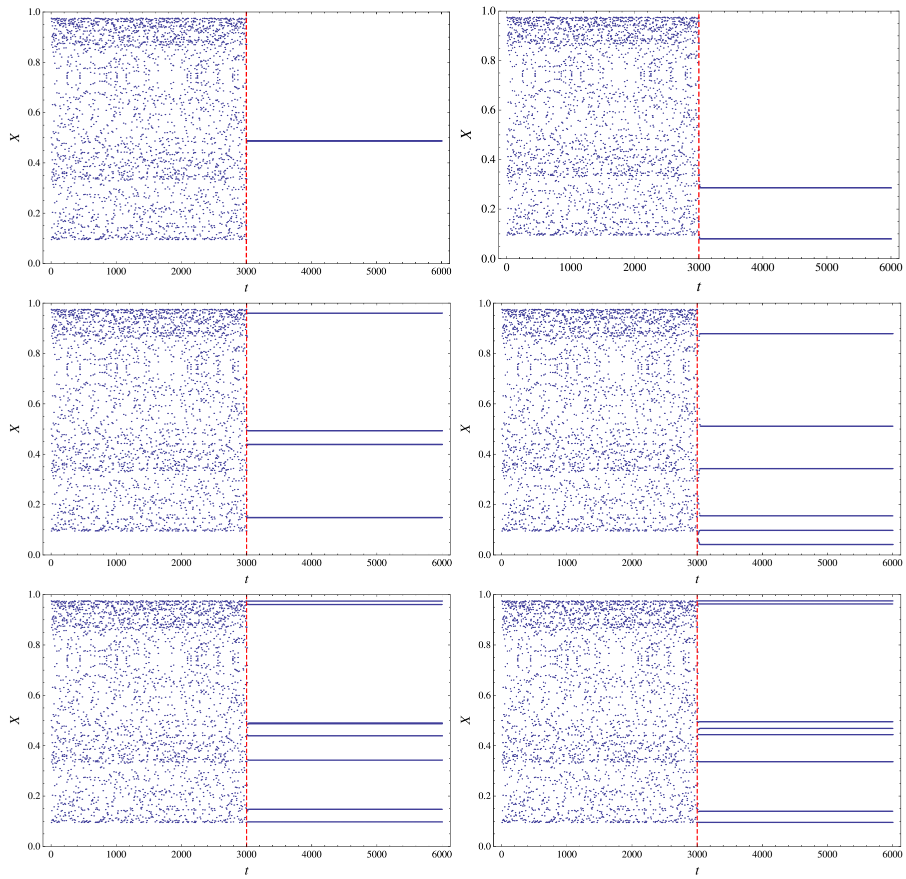

Fig. 5. (top-bottom, left-right) Six examples of application of our method for the logistic map and the parameter value $a = 3.9$: (t-l) period-1 orbit; (t-r) period-2 orbit; (m-l) period-4 orbit; (m-r) period-6 orbit; (b-l) period-7 orbit; (b-r) period-8 orbit.

bits of this figure. This is a clear evidence of the strong sensitivity to the initial conditions of the logistic map.

5.3 Case 3: parameter value $r = 3.8$

Figure 4 shows six additional examples for the parameter value $a = 3.8$, corresponding to period 1, 2, 4, and 6 orbits selected as targets. Interestingly, two examples are shown for the period-4 and period-6 orbits, showing that our optimization problem is multimodal, as different combinations of values for the pulse intensity and frequency can lead to periodic orbits of the same period. Note also that similar values of the parameter λ can still lead to orbits of different periods, depending on the value of Δn. This is the case for the period-1, period-4 and period-6 orbits in this figure, which are obtained for the same value $\lambda = -0.45$

ICCS Camera Ready Version 2025
To cite this paper please use the final published version:
DOI: 10.1007/978-3-031-97564-6_17

but with different pulse frequencies $\Delta n = 1$, $\Delta n = 2$, and $\Delta n = 3$, respectively. Similarly, the same value of Δn can lead to orbits of different periods depending on the value of λ. This is the case for the period-2 and period-4 orbits in Fig. 4, obtained for the same value $\Delta n = 2$ but with different pulse intensities $\lambda = -0.9$ and $\lambda = -0.45$, respectively. Finally, two different period-6 orbits have been obtained for the same pulse frequency $\Delta n = 3$, but with different pulse intensities $\lambda = -0.45$ and $\lambda = -0.9$, respectively. This shows the high diversity of different behaviors that can be obtained with our method. Note that the difference in the pulse intensity leads to a shifted region of the period-6 orbit in Fig. 4(bottom-right) with respect to the period-6 orbit in Fig. 4(bottom-left) and also with respect to the original chaotic attractor before the chaos control method is applied.

5.4 Case 4: parameter value $r = 3.9$

Figure 5 shows six examples of the application of our chaos control method for the parameter value $a = 3.9$, corresponding to period 1, 2, 4, 6, 7, and 8 orbits. They have been obtained for different combinations of λ and Δn reported in the last two columns of Table 1. It is interesting to remark that three different periodic behaviors have been attained for the same pulse frequency $\Delta n = 4$ and close values of the pulse intensity: $\lambda = -0.55$, $\lambda = -0.52$, and $\lambda = -0.49$ for period-4, period-7 and period-8 orbits, respectively. In practical terms, this $\Delta n = 4$ value of the pulse frequency implies that the effective pulse intensity is actually much smaller for each individual iteration. However, even these small variations of the pulse intensity can result in different periodic behaviors.

6 Conclusions and Future Work

In this paper, we address the problem of chaos control, which involves stabilizing the chaotic behavior of a dynamical system to a periodic orbit with a prescribed period. The chaos control considered in this work is based on the application of multiplicative pulses of intensity λ on the system variables every Δn iterations, with λ and Δn being method parameters. This problem is formulated as a difficult multimodal multivariate continuous nonlinear optimization problem. This optimization problem is addressed through a popular swam intelligence method called bat algorithm that is applied to compute the relevant parameters of the chaos control procedure. We conducted computational experiments to evaluate the performance of our approach, applying it to several illustrative examples with different parameter values of the logistic map. The experimental results demonstrate that the method performs effectively, successfully stabilizing chaotic behavior into periodic orbits of various periods. We conclude that this method shows promise as a fully automatic procedure for chaos control in chaotic maps.

Despite the positive results, our method does have some limitations. For instance, we were unable to automatically obtain certain periodic behaviors (e.g.,

ICCS Camera Ready Version 2025
To cite this paper please use the final published version:
DOI: 10.1007/978-3-031-97564-6_17

period-11 orbits). We suspect that they correspond to very narrow windows of the parameter r, making them challenging to capture within the number of iterations considered in our method. Expanding our approach to address such cases is a goal for future research. Additionally, we plan to extend our method to chaotic maps of higher dimensions and to tackle the more complex case of continuous chaotic systems (flows), cases that present additional complexity [9]. We also aim to conduct a comparative analysis with other artificial intelligence-based methods as part of our future work in the field. Finally, we wish to investigate the application of this control of chaos technique to other interesting problems in dynamical systems, such as the synchronization of chaotic systems [11, 17, 29] and their potential role for secure communications.

Acknowledgment

The authors thank the financial support from the project PDE-GIR of the European Union's Horizon 2020 research and innovation programme, in the Marie Sklodowska-Curie Actions programme, with grant agreement of reference number 778035, and also from the Agencia Estatal de Investigación (AEI) of the Spanish Ministry of Science and Innovation (Computer Science National Program), for the grant of reference number PID2021-127073OB-I00 of the MCIN/AEI/10.13039/501100011033/FEDER, EU.

References

1. G.L. Baker, J.P. Gollub, *Chaotic Dynamics: An Introduction*. Cambridge University Press, Cambridge, UK, 1990.
2. C.S. Bertuglia, F. Vaio, *Nonlinearity, Chaos, and Complexity: The Dynamics of Natural and Social Systems*. Oxford University Press, Oxford, UK, 2005.
3. W.M. Bessa, A.S. De Paula, M. A. Savi, Chaos control using an adaptive fuzzy sliding mode controller with application to a nonlinear pendulum.Chaos, Solitons and Fractals, 42(2), pp. 784–791, 2009.
4. S. Boccaletti, C. Grebogi, Y.-C. Lai, H. Mancini, D. Maza, The control of chaos: theory and applications. Physics Reports, 329, pp. 103–197, 2000.
5. A.S. De Paula, M.A. Savi, A multiparameter chaos control method based on OGY approach. Chaos, Solitons and Fractals, 40(3), pp. 1376–1390, 2009.
6. A.S. De Paula, M.A. Savi, Comparative analysis of chaos control methods: A mechanical system case study. International Journal of Non-Linear Mechanics, 46, pp. 1076–1089, 2011.
7. R.L. Devaney, *An Introduction to Chaotic Dynamical Systems, Third Edition*. CRC Press, Boca Raton, FL, 2022.
8. A.L. Fradkov, R.J. Evans, B.R. Andrievsky, Control of chaos: methods and applications in mechanics. Philosophical Transactions of the Royal Society A 364, pp. 2279–2307, 2006.
9. A. Gálvez, Numerical-symbolic Matlab program for the analysis of three-dimensional chaotic systems. Proc. of International Conference on Computational Science – ICCS 2005, Lecture Notes in Computer Science, 4488. Springer, Berlin, Heidelberg, 211–218, 2007.

ICCS Camera Ready Version 2025
To cite this paper please use the final published version:
DOI: 10.1007/978-3-031-97564-6_17

10. A. Gálvez, I. Fister Jr., E. Osaba, I. Fister, J.D. Ser, A. Iglesias, Computing rational border curves of melanoma and other skin lesions from medical images with bat algorithm. *Proc. Genetic and Evolutionary Computation Conf., ACM GECCO 2019*, ACM, pp. 1675-1682, 2019.
11. A. Gálvez, A. Iglesias, Symbolic/numeric analysis of chaotic synchronization with a CAS, *Future Generation Computer Systems*, 23 (5), 727–733, 2007.
12. A. Gálvez, A. Iglesias, J.A. Díaz, I. Fister, J. López, I. Fister Jr., Modified OFS-RDS bat algorithm for IFS encoding of bitmap fractal binary images. *Advanced Engineering Informatics*, vol. 47, Paper 101222, 2021.
13. A. Gálvez, A. Iglesias, E. Osaba, J. del Ser, Bat algorithm method for automatic determination of color and contrast of modified digital images. *Prof. of 44th Annual Computers, Software, and Applications Conference, IEEE COMPSAC 2020*, pp. 1195–1200, 2020.
14. A. Gálvez, S. Pérez-Carabaza, A. Iglesias, Bat algorithm for attractor reconstruction of low-dimensional chaotic maps from time series. Proc. of 2024 IEEE 48th Annual Computers, Software, and Applications Conference (COMPSAC). IEEE, 1642–1647, 2024.
15. J. Güémez, J.M. Gutiérrez, A Iglesias, M.A. Matías, Stabilization of periodic and quasiperiodic motion in chaotic systems through changes in the system variables. *Physics Letters A*, 190 (5-6), 429–433, 1994.
16. J. Güémez, J.M. Gutiérrez, A Iglesias, M.A. Matías, Suppression of chaos through changes in the system variables: transient chaos and crises. *Physica D: Nonlinear Phenomena*, 79 (2-4), 164–173, 1994.
17. J.M. Gutiérrez, A. Iglesias, Synchronizing chaotic systems with positive conditional Lyapunov exponents by using convex combinations of the drive and response systems, *Physics Letters A*, 239(3), 174–180, 1998.
18. J.M. Gutiérrez, A. Iglesias, A Mathematica package for the analysis and control of chaos in nonlinear systems, *Computers in Science and Engineering*, 12 (6), 608–619, 1998.
19. J.M. Gutiérrez, A Iglesias, J Güémez, M.A. Matías, Suppression of chaos through changes in the system variables through Poincaré and Lorenz return maps, *International Journal of Bifurcation and Chaos*, vol. 6, Issue 7, pp. 1351–1362, 1996.
20. R. Hilborn, *Chaos and Nonlinear Dynamics: An Introduction for Scientists and Engineers*. Oxford University Press, Oxford, UK, 2001.
21. B. Hübinger, R. Doerner, W. Martienssen, M. Herdering, R. Pitka, U. Dressler, Controlling chaos experimentally in systems exhibiting large effective Lyapunov exponents. Physical Review E, 50(2), pp. 932–948, 1994.
22. A. Iglesias, J.M. Gutiérrez, J. Güémez, M.A. Matías, Chaos suppression through changes in the system variables and numerical rounding errors, *Chaos, Solitons and Fractals*, vol. 7, Issue 8, pp. 1305–1316, 1996.
23. A. Iglesias, A. Gálvez, M. Collantes, Bat algorithm for curve parameterization in data fitting with polynomial Bézier curves. Proc. of 2015 International Conference on Cyberworlds (CW). IEEE, 107–114, 2015.
24. A. Iglesias, A. Gálvez, M. Collantes, Multilayer embedded bat algorithm for B-spline curve reconstruction. *Integrated Computer-Aided Engineering*, vol. 24(4), pp. 385–399, 2017.
25. A. Iglesias, A. Gálvez, M. Collantes, Iterative sequential bat algorithm for free-form rational Bézier surface reconstruction. *International Journal of Bio-Inspired Computation*, vol. 11(1), pp. 1–15, 2018.
26. T. Kapitaniak, Controlling chaotic oscillators without feedback. *Chaos, Solitons and Fractals*, 2(5), pp. 512–530, 1992.

ICCS Camera Ready Version 2025
To cite this paper please use the final published version:
DOI: 10.1007/978-3-031-97564-6_17

27. R.J. Korte, J.C. de Schouten, C.M. van den Bleek, Experimental control of a chaotic pendulum with unknown dynamics using delay coordinates. Physical Review E52(4), pp. 3358–3365, 1995.
28. E. Ott, C. Grebogi, J.A. Yorke, Controlling chaos, Physical Review Letters, 64 (11), pp. 1196–1199, 1990.
29. L.M. Pecora, T.L. Carroll, Synchronization in chaotic systems. *Physical Review Letters*, vol. 64, pp. 821–823, 1990.
30. F.H.I. Pereira-Pinto, A.M. Ferreira, M.A. Savi, Chaos control in a nonlinear pendulum using a semi-continuous method. Chaos, Solitons and Fractals, 22 (3), pp. 653–668, 2004.
31. K. Pyragas, Continuous control of chaos by self-controlling feedback, Physics Letters, A170, pp. 421–428, 1992.
32. K. Pyragas, Delayed feedback control of chaos, Philosophical Transactions of the Royal Society A, 364, pp. 2309–2334, 2006.
33. M.A. Savi, F.H.I. Pereira-Pinto, A.M. Ferreira, Chaos control in mechanical systems. Shock and Vibration, 13, pp. 301–314, 2006.
34. H. G. Schuster, *Deterministic Chaos. An Introduction.* VCH, 1988.
35. T. Shinbrot, C. Grebogi, E. Ott, J.A. Yorke, Using small perturbations to control chaos. Nature, 363, pp. 411–417, 1993.
36. J.E.S. Socolar, D.W. Sukow, D.J. Gauthier, Stabilizing unstable periodic orbits in fast dynamical systems. Physical Review E, 50(4), pp. 3245–3248, 1994.
37. P. Suárez, A. Iglesias, Bat algorithm for coordinated exploration in swarm robotics. *Prof. of 8th Int. Conf. ICSI 2017*, pp. 176–184, 2017.
38. P. Suárez, A. Iglesias, A. Gálvez, Autonomous coordinated navigation of virtual swarm bots in dynamic indoor environments by bat algorithm. *Prof. of 3rd Int. Conf. ICHSA 2017*, pp. 134–144, 2017.
39. P. Suárez, A. Iglesias, A. Gálvez, Make robots be bats: specializing robotic swarms to the bat algorithm. *Swarm and Evolutionary Computation*, vol. 44, pp. 113–129, 2019.
40. J.M.T. Thompson, H.B. Stewart, *Nonlinear Dynamics and Chaos, 2nd ed.*, John Wiley & Sons, Hoboken, NJ, 2002.
41. X.S. Yang, A new metaheuristic bat-inspired algorithm. *Studies in Computational Intelligence*, Springer Berlin, vol. 284, pp. 65–74, 2010.
42. X.S. Yang, Bat algorithm: literature review and applications. *Int. Journal of Bio-Inspired Computation*, vol. 5(3), pp. 141–149, 2013.
43. X.S. Yang, A.H. Gandomi, Bat algorithm: a novel approach for global engineering optimization. *Engineering Computations*, vol. 29(5), pp. 464–483, 2012.

ICCS Camera Ready Version 2025
To cite this paper please use the final published version:
DOI: 10.1007/978-3-031-97564-6_17